crystals

MDPI

Article

Observation of a New Polyhalide Phase in Ag-Cl_2 System at High Pressure

Adam Grzelak [1,*], Jakub Gawraczyński [1], Mariana Derzsi [2], Viktor Struzhkin [3], Maddury Somayazulu [4] and Wojciech Grochala [1]

1 Center of New Technologies, University of Warsaw, 02-089 Warsaw, Poland; j.gawraczynski@cent.uw.edu.pl (J.G.); w.grochala@cent.uw.edu.pl (W.G.)
2 Advanced Technologies Research Institute, Faculty of Materials Science and Technology in Trnava, Slovak University of Technology in Bratislava, 917 24 Trnava, Slovakia; mariana.derzsi@gmail.com
3 Center for High Pressure Science and Technology Advanced Research, Shanghai 201203, China; viktorstruzhkin@yahoo.com
4 HPCAT, X-ray Science Division, Argonne National Laboratory, Lemont, IL 60439, USA; zulu@anl.gov
* Correspondence: a.grzelak@cent.uw.edu.pl

Abstract: In this short contribution, we examine Raman spectroscopic data from high-pressure and high-temperature experiments with an Ag-Cl_2 system, and find that they are in good agreement with previously observed and calculated spectra of polychloride species. Our results imply the formation of a hitherto unknown $AgCl_x$ compound, which warrants further study.

Keywords: silver; polyhalides; high pressure

check for updates

Citation: Grzelak, A.; Gawraczyński, J.; Derzsi, M.; Struzhkin, V.; Somayazulu, M.; Grochala, W. Observation of a New Polyhalide Phase in Ag-Cl_2 System at High Pressure. *Crystals* **2021**, *11*, 1565. https://doi.org/10.3390/cryst11121565

Academic Editors: Jesús Prado-Gonjal, Beatriz Molero-Sánchez and Sara A. López-Paz

Received: 15 November 2021
Accepted: 13 December 2021
Published: 15 December 2021

Publisher's Note: MDPI stays neutral with regard to jurisdictional claims in published maps and institutional affiliations.

Copyright: © 2021 by the authors. Licensee MDPI, Basel, Switzerland. This article is an open access article distributed under the terms and conditions of the Creative Commons Attribution (CC BY) license (https://creativecommons.org/licenses/by/4.0/).

1. Introduction

Among the three coinage metals known since antiquity—copper, silver and gold—the chemistry of silver is perhaps the most elusive and challenging [1]. It adopts the oxidation state +1 (with closed-subshell d^{10} electronic configuration) in the vast majority of its known compounds [1]. However, it is the chemistry of silver(II) that has received greater attention from solid state chemists and physicists, due to the unpaired d electron giving rise to magnetic interactions in AgF_2 and its ternary derivatives [2,3]. Ag^{2+} cation is also one of the strongest known oxidizers and because of that, it is found predominantly in the coordination environment of fluorine (the most electronegative element) as the ligand in known compounds of Ag^{II}.

In this work, we are concerned with the possibility of obtaining novel combinations of silver and chlorine (the third most electronegative element). Phase diagram of binary Ag/Cl system features only one stable compound—silver(I) chloride AgCl (a well-known photosensitive agent in traditional photography). There exists a variety of other compounds containing silver and chlorine, e.g., ionic conductors Ag_5Te_2Cl [4] or $AgF_{1-x}Cl_x$ [5], complex chlorides such as $Ag[AuCl_4]$ [6] and $Ag[AlCl_4]$ [7], or even ternary chloroargentates, such as $CsAgCl_2$ [8,9], Cs_2AgCl_3 [9], and Rb_2AgCl_3 [9,10]. All of the above, however, feature silver in the oxidation state +1—as does AgCl. An interesting example can be found in the case of $Cs_2Ag^{I}Ag^{III}Cl_6$—a mixed-valence chloroargentate with a perovskite-like structure, in which Ag centers are coordinated by Cl atoms in compressed (for Ag^{I}) or elongated (for Ag^{III}) octahedra [11]. The latter compound serves as an example of charge-transfer instability of Ag^{II} species in homoleptic environment of ligands less electronegative than fluorine, evidenced also by the case of $Ag^{I}Ag^{III}O_2$ [12,13], which has been found to retain its mixed-valent (and insulating) character even when compressed to 80 GPa [14]. This tendency, along with the aforementioned high reactivity of Ag^{II} species (towards ligands less electronegative than fluorine), can be used to explain the scarcity of known $AgCl_x$ compounds. Nevertheless, a possibility of obtaining novel binary silver chlorides has been investigated computationally in recent years. Our previous studies have looked

at the relative stability of various structural candidates for $AgCl_2$ [15], and a different work has identified a candidate structure for a silver subchloride [16]. All of the aforementioned compounds or polymorphs turn out to be metastable with respect to decomposition into AgCl. However, the list of possible candidates for new $AgCl_x$ combinations is not exhausted by the aforementioned studies. As another example of possible configurations, one can mention recently discovered higher chlorides of sodium [17,18] and potassium [19]. The ionic radius of Ag^I is similar to that of Na^I [20] and thus chemistry of their respective polychlorides could also be similar. Indeed, we argue that the experimental data obtained and reported in this contribution points to formation of a hitherto unknown compound, which contains Ag^I and polychloride Cl_x^- anions [21].

2. Materials and Methods

High-pressure experiments involving mixtures of Ag or AgCl with Cl_2 were performed using a diamond-anvil cell (DAC) supplied by Almax EasyLab (Diksmuide, Belgium), with diamond culets 250 μm in diameter. Gaskets were prepared as follows: a rhenium gasket blank was indented to ca. 10 GPa (using ruby fluorescence as pressure gauge [22]), after which a hole ca. 100 μm in diameter was cut out using an infrared laser. A cylinder-shaped piece of hastelloy, matching in size, was inserted into the hole and welded together with the rhenium gasket through further compression, after which a hole was again cut out. The gasket was placed on one of the seats of the DAC and fit tightly to the diamond anvil using a Seger ring. A thin layer of alumina (Al_2O_3) was deposited on parts of the gasket in contact with diamond facets, in order to avoid sliding of the gasket lubricated by Cl_2. (These parts were not in contact with the sample chamber.) Gaseous Cl_2 was then loaded from a capillary into the gasket hole while the entire system was being cooled in liquid nitrogen inside an argon-filled glove-box with desiccant, in order to ensure condensation of chlorine uncontaminated by moisture. Ag or AgCl (depending on the experiment) was loaded by placing a microcrystalline sample on the other diamond anvil.

Raman spectra were collected using a 532 nm laser. Pressure in samples was determined using the high-edge frequency of first-order Raman band of diamond from diamond anvil [23]. Infrared laser was used in selected experiments to heat the studied Ag-Cl_2 sample.

Complementary density functional theory (DFT) calculations were carried out using VASP software [24–28], with GGA-type Perdew-Burke-Ernzerhof functional adapted for solids (PBEsol) [29]. More detailed description of settings can be found in Supplementary Materials.

3. Results

We performed several runs of compression experiments with either Ag or AgCl loaded together with Cl_2 into a DAC. In general, assuming no reaction taking place, we expect the Raman spectrum to be dominated by features originating from Cl_2—a molecular crystal (chlorine solidifies at room temperature at pressure as low as 1.45 GPa [30]). AgCl, as an ionic solid with rocksalt structure at ambient pressure, would likely produce only relatively low-intensity overtone bands below 400 cm^{-1} at ambient pressure [31,32]. In addition, AgCl undergoes a series of phase transitions in the range 7–13 GPa, ultimately leading to CsCl-type polymorph [33]. Although Raman spectra of CsCl-type AgCl have not been reported, selection rules indicate that only the overtone of IR-active T_{1u} mode can be Raman-active, as is the case with isostructural AgF at high pressure [34]. We simulated the pressure dependence of those frequencies using DFT calculations for reference in further discussion (methodology and results are shown in Supplementary Materials). Similarly, Ag, as a metal with fcc crystal structure, is not expected to produce any Raman signal at all. Accordingly, in one of the experiments—where we compressed AgCl with Cl_2 and measured Raman spectra at various pressure points between 8 and 52 GPa (initially without any laser heating), we observed bands characteristic of solid Cl_2, whose frequencies and pressure dependence were previously reported by Johannsen et al. [35].

In Figure 1, we plot chlorine band frequencies measured in this work as a function of pressure. Overall, our results for chlorine are in very good agreement with previously reported data [35], although we extended our assignment to bands appearing in the region up to ca. 1100 cm^{-1}. We present example spectra and more detailed assignment in Supplementary Materials. For the purpose of this work, signals originating from Cl_2 serve as a backdrop for identification of additional bands, which were observed in further experiments, as discussed below.

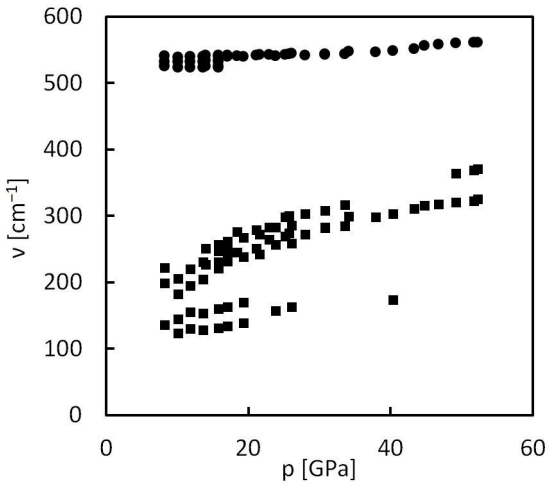

Figure 1. Pressure dependence of bands identified as originating from solid molecular chlorine, taken from one of the experimental runs. Based on ref. [35], we assign these bands as: squares—lattice phonons, circles—intramolecular Cl-Cl vibrations. (More detailed information on the assignment can be found in Supplementary Materials).

We performed two other experimental runs: (A) AgCl + Cl_2 mixture compressed to ca. 40 GPa, laser-heated several times and further compressed to ca. 60 GPa in several steps, and (B) Ag + Cl_2 mixture compressed initially to ca. 4 GPa and further compressed to ca. 27 GPa in several steps, without laser heating. Raman spectra were collected at each compression step in both samples.

In Figure 2, we present spectra collected for sample A. The two most prominent ones can be assigned to chlorine as Cl-Cl vibron (at ca. 550 cm^{-1} at 42 GPa) and as A_g lattice phonon (at ca. 310 cm^{-1} at 42 GPa). The lower-intensity signal in the range 350–390 cm^{-1} (depending on pressure) is most likely the B_{3g} solid Cl_2 lattice phonon. In the higher-frequency region, the previously mentioned overtone of Cl-Cl vibron is also visible at 1070–1090 cm^{-1}. Importantly, we can discern several new bands appearing in the range just below the Cl-Cl vibron (400–500 cm^{-1}). The bands are relatively weak, but repeatable, and the spectrum is still dominated by features from Cl_2. Several weak signals can also be discerned in the higher-frequency region (600–1000 cm^{-1}). It is important to stress that these new bands appeared after laser-heating and therefore cannot be assigned to AgCl or to any other constituent present in DAC from the beginning. Overtone bands which could originate from CsCl-type AgCl (cf. Supplementary Materials) are not observed in the spectrum, indicating very low Raman activity of this system.

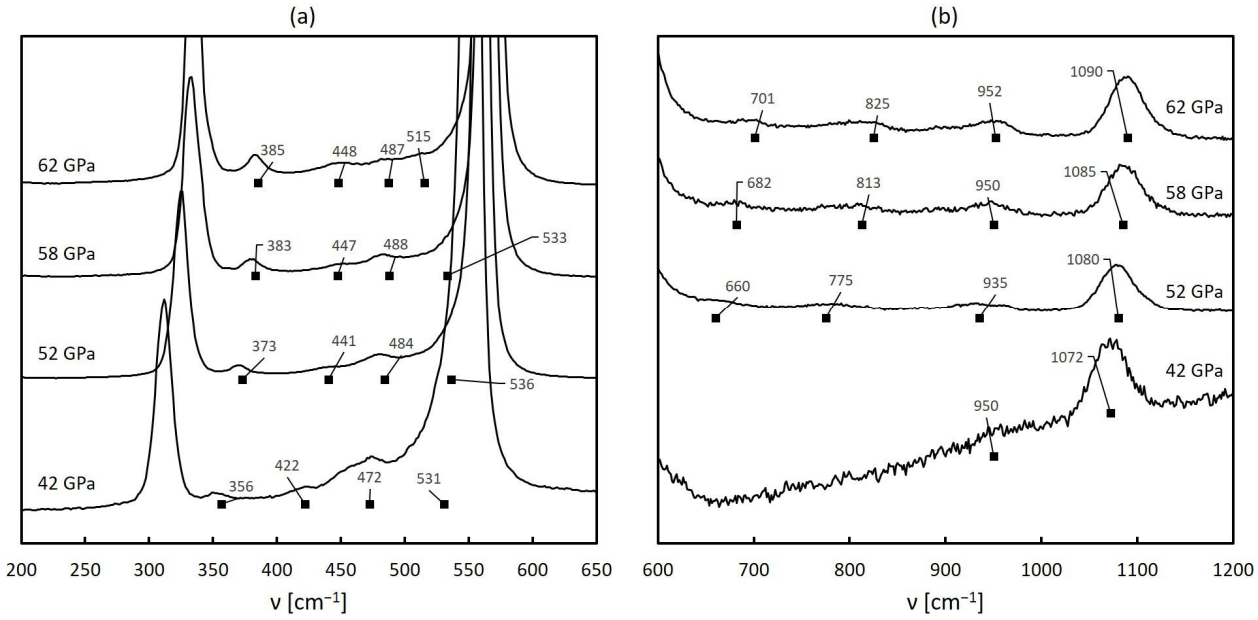

Figure 2. Comparison of spectra obtained in experiment A: AgCl + Cl_2 mixture compressed initially to ca. 40 GPa and laser-heated. (**a**) 200–650 cm^{-1} range, (**b**) 600–1200 cm^{-1} range. See text for further details.

Raman spectra collected from experiment B are shown in Figure 3. In this case, we can also observe new bands appearing in the 400–500 cm^{-1} region. Interestingly, this occurs in sample B even without laser heating. Assuming that the origin of these new signals is a product of reaction in the Ag-Cl_2 system, such observation is not surprising—we can expect that the activation barrier for the reaction between metallic Ag and Cl_2 will be lower than for the respective reaction of AgCl and Cl_2, since AgCl is thermodynamically stable with respect to Ag and Cl_2 at room temperature within the studied pressure range [33]. The possible origin of new bands appearing in Figures 2 and 3 is discussed below.

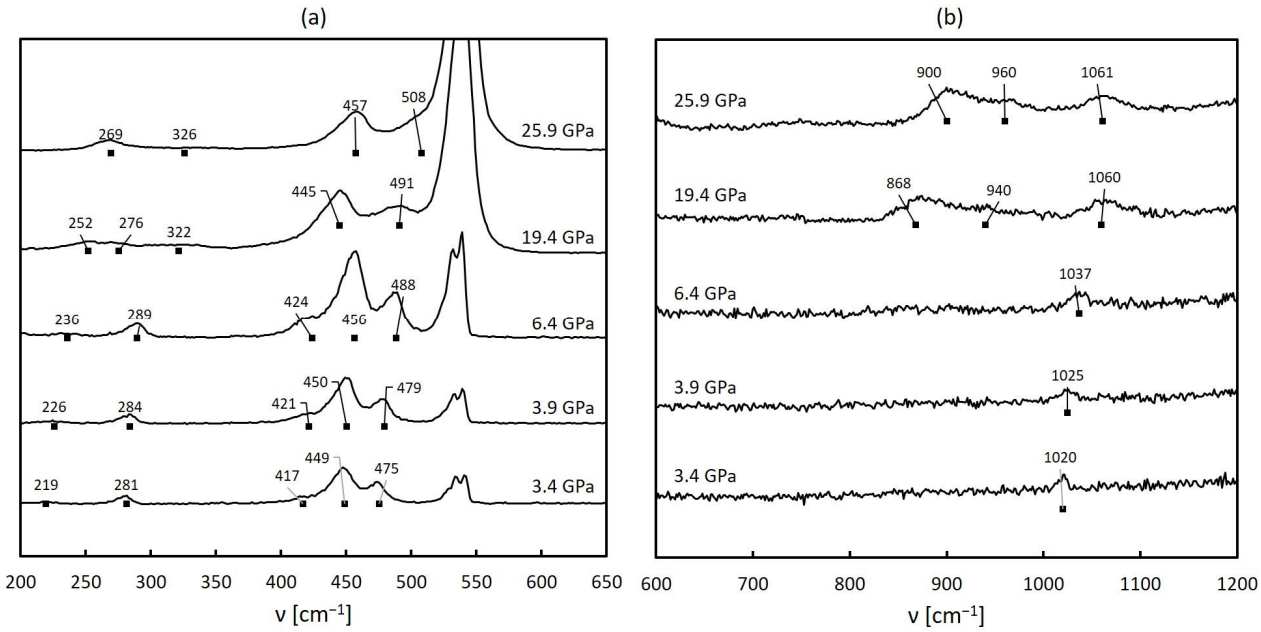

Figure 3. Comparison of spectra obtained in experiment B. Ag + Cl_2 mixture compressed initially to ca. 3 GPa. (**a**) 200–650 cm^{-1} range, (**b**) 600–1200 cm^{-1} range. See text for further details.

The appearance of bands which cannot be assigned to any of the constituents of the initial mixture clearly indicate that a reaction has taken place. The system Ag/AgCl

+ Cl_2 can in principle also interact with the gasket material (hastelloy, a material made up mostly of Ni, Cr and Mo) and the diamond anvil, particularly in the heated samples. However, we have chosen hastelloy as a gasket material due to its chemical resistance, and the reaction between it and Cl_2 (especially without laser heating) appears unlikely. Known spectral data for possible products of such reaction, i.e., nickel, chromium, and molybdenum chlorides, also testify against such assignment of the new bands in the 400–500 cm^{-1} region [36–38]. Furthermore, a reaction between Cl_2 and diamond could conceivably occur, although previous experimental works with similar setup and heating do not mention such outcome [39]. Chlorinated diamond surfaces have been analyzed by Raman spectroscopy [40]; C-Cl vibrations in such systems are expected to fall in the 600–800 cm^{-1} range. In this work, a faint band appearing in sample A between 660 and 700 cm^{-1} may originate from such vibrations. Its intensity is very weak and thus the extent of such chlorination can be considered very low, if it occurs at all. Finally, CCl_4 could in principle be another product of reaction between diamond and Cl_2. Raman spectra and phase transitions of CCl_4 have been previously studied, and known frequencies of its bands from those works have been taken into account when analyzing new bands in experiments A and B [41].

Figures 4 and 5 plot pressure dependence of new bands observed in samples A and B, together with previously reported bands of CCl_4 [41]. Although the range of data for CCl_4 is only up to ca. 30 GPa, we can still see that the new bands in 400–500 cm^{-1} cannot be accounted for by this compound. Several of the higher-frequency bands (in 600–1200 cm^{-1}) can be assigned to Cl_2 vibron overtones and to combination modes mentioned previously. The bands in the 850–950 cm^{-1} region, regardless of their chemical origin, are likely overtones of the bands between 400 and 500 cm^{-1}, since in general, overtones are a common occurrence in Raman spectroscopy (cf. Supplementary Materials for assignment of overtones and combination modes in Cl_2 spectrum). Overtones tend to be strong when Raman spectra have resonance character, which is quite likely in the case of the dark brown sample (cf. Supplementary Materials) illuminated with a visible laser beam.

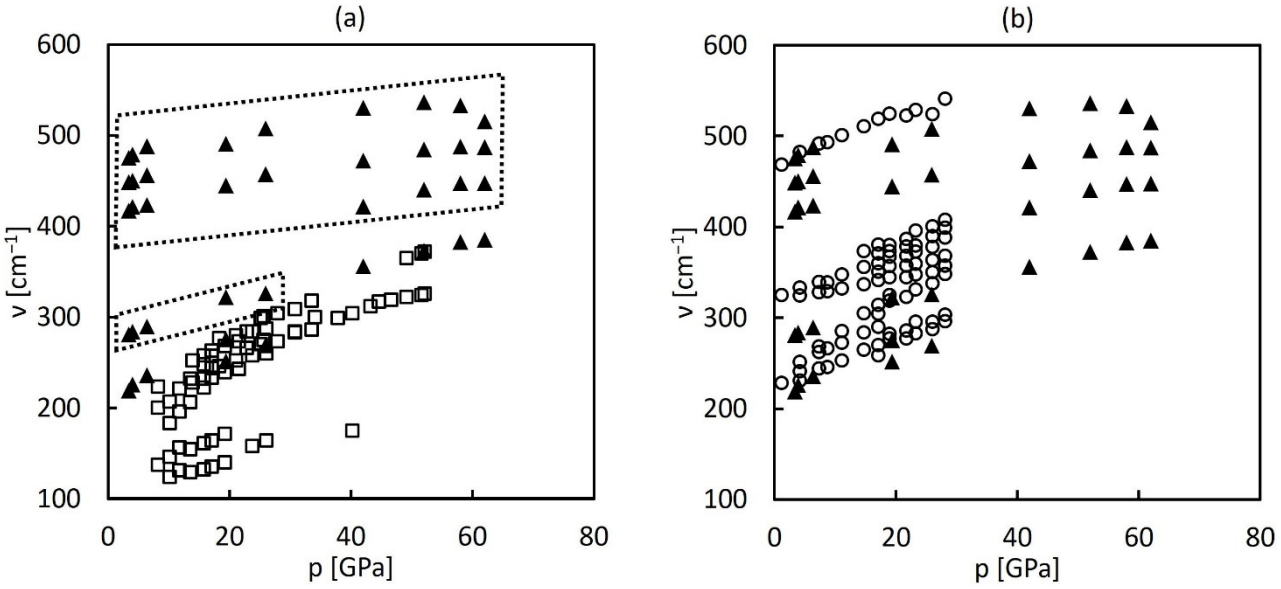

Figure 4. Comparison of new bands appearing in spectra from experiments A and B (solid triangles) with: (**a**) known bands from solid chlorine (this work, hollow squares), (**b**) known bands from solid CCl_4 (ref. [41], hollow circles). Cl-Cl intramolecular vibron band appearing at 550–600 cm^{-1} is omitted for clarity. Dashed parallelograms indicate bands unaccounted for by Cl_2 or CCl_4. Reproduced with permission from ref. [41]. Copyright 2014 AIP Publishing.

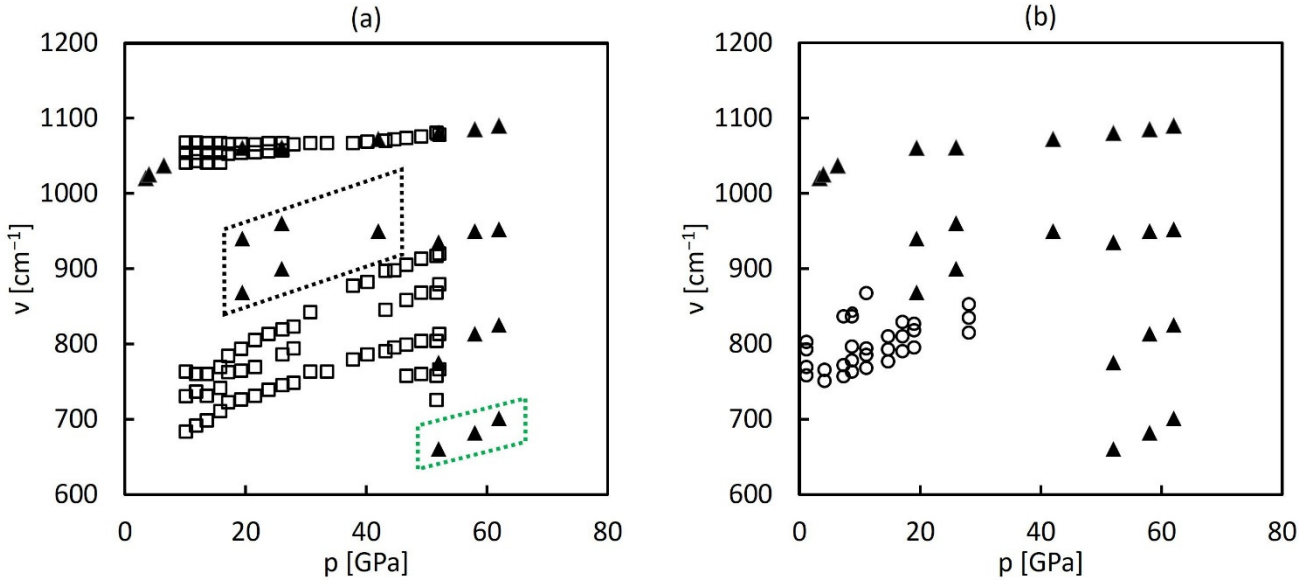

Figure 5. Comparison of new bands appearing in spectra from experiments A and B (solid triangles) with: (**a**) known bands from solid chlorine (this work, hollow squares), (**b**) known bands from solid CCl_4 (ref. [41], hollow circles). Black dashed parallelogram indicates bands unaccounted for by Cl_2 or CCl_4. Green dashed parallelogram indicates bands possibly originating from chlorinated diamond. Reproduced with permission from ref. [41]. Copyright 2014 AIP Publishing.

4. Discussion

Having ruled out possible candidates for undesirable reaction products, we can attempt to determine the identity of system constituents which give rise to the new bands in the 400–500 cm^{-1} region. Discontinuities in pressure dependence and relative positions of these bands (Figures 4 and 5) between sets A and B suggest that they may belong either to different polymorphs of the same compound (obtained as one phase in experiment A and as another in B) or to different compounds altogether. These bands are located just below the dominant Cl-Cl vibron band, and simple considerations based on the harmonic oscillator model indicate that they could originate from: (a) X-Cl vibrations, where X is an atom heavier that Cl, (b) Cl-Cl vibrations from a species featuring Cl-Cl bonds longer than in Cl_2 molecule, such as polychloride anions [42–44], or (c) a lattice phonon in a solid compounds featuring (a) and/or (b). Figure 6 shows the spectrum obtained for sample B at 3.9 GPa, and compares it with simulated spectra of example polychloride species at ambient pressure, with frequencies taken from refs. [42,43]. While not an exact match, it is worth noting that (i) these values were observed/calculated for different compounds containing complex organic cations, so we can expect these frequencies to vary to some extent depending on the system, and (ii) there is no data on the pressure dependence of Raman spectra of polychlorides, so a certain discrepancy (a positive shift) can be expected between previously reported values and spectra presented in this work. However, the comparison in Figure 6 gives strong credibility to the hypothesis that polychloride species such as Cl_5^- or Cl_9^- are indeed present in the sample. Lastly, the sample obtained in experiment A turned visibly brown at the irradiation spot (cf. Supplementary Materials, Figure S6), which indicates formation of a product with a charge-transfer transition in the visible range. Given that Ag(I) polychloride(s) is/are present in the sample, the transition responsible for the color may correspond to metal-to-ligand charge transfer excitation from occupied d states in Ag^I and empty σ* antibonding states in Cl_2 molecule within polychloride anion or array (Ag^I d → Cl_2 σ*).

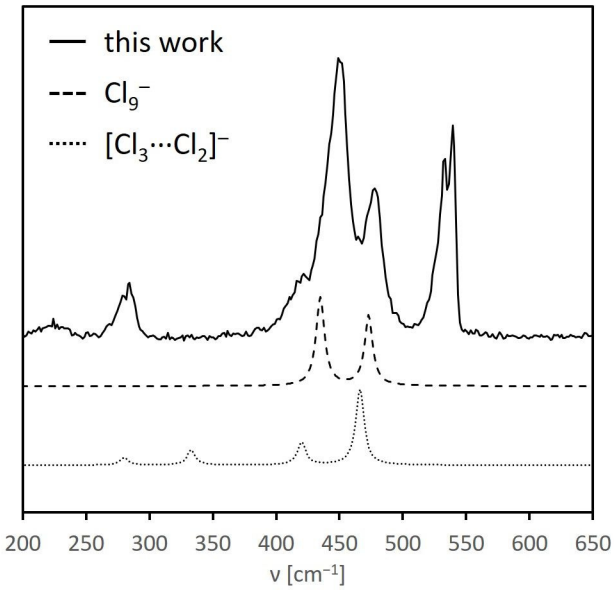

Figure 6. Comparison of the 200–600 cm^{-1} region of sample B spectra at 3.9 GPa with Raman bands of polychloride anions derived from ref. [42] for Cl_9^- anion and from ref. [43] for 2D polychloride network. Relative intensities are also adapted from cited works.

5. Conclusions

We have obtained and analyzed Raman spectra probing several experiments with binary Ag-Cl_2 system, and we argue that the data is indicative of the formation of an as-yet unknown phase or phases. Based on the positions of new Raman bands observed in the experiments, these new phase(s) most likely contain polychloride anions [42] or in general, a more complex arrangement of Cl atoms [43]. Recent computational work investigating different stoichiometries of $AgCl_x$ compounds using evolutionary algorithm has indeed pointed to a possibility of formation of polymorphs with polychloride anions for $x > 2$ [45]. A common feature emerging in those solutions are Cl_3^- anions, and $[Cl_3 \ldots Cl_2]^-$ or $[Cl_2 \ldots Cl_2]^-$ infinite networks. Further study is needed in order to elucidate the exact nature of reaction products reported here. Unfortunately, high-pressure synchrotron X-ray diffraction measurements, which could provide insight into the crystal structure of these systems, have been severely delayed due to the ongoing COVID-19 pandemic.

Supplementary Materials: The following are available online at https://www.mdpi.com/article/10.3390/cryst11121565/s1, S1: Raman spectra of solid Cl_2 and pressure dependence of band frequencies, S2: Pressure dependence of simulated (DFT) frequencies of the overtone of IR-active T_{1u} mode of AgCl in CsCl structure, S3: Picture of the one of the samples.

Author Contributions: A.G. and J.G. performed the experiments. V.S. and M.S. supervised the experiments. A.G. and M.D. performed complementary DFT calculations. A.G., J.G., M.D. and W.G. analyzed the results. M.D. and W.G. reviewed the manuscript. All authors have read and agreed to the published version of the manuscript.

Funding: This work was financed by the Polish National Science Center (NCN) through a Preludium grant (2017/25/N/ST5/01976). M.D. acknowledges the ERDF, Research and Innovation Operational Programme (ITMS2014+: 313011W085), the Slovak Research and Development Agency (APVV-18-0168), and Scientific Grant Agency of the Slovak Republic (VG 1/0223/19).

Data Availability Statement: Experimental data (Raman spectra) are available from the corresponding author upon request.

Acknowledgments: A.G. would like to thank Przemysław Malinowski (Center of New Technologies, UW) and Dominik Kurzydłowski (Faculty of Mathematics and Natural Sciences, UKSW) for their help in preparing and carrying out the experiments.

Conflicts of Interest: The authors declare no conflict of interest.

References

1. Grochala, W. Silverland: The Realm of Compounds of Divalent Silver—And Why They are Interesting. *J. Supercond. Nov. Magn.* **2017**, *31*, 737–752. [CrossRef]
2. Gawraczyński, J.; Kurzydłowski, D.; Ewings, R.A.; Bandaru, S.; Gadomski, W.; Mazej, Z.; Ruani, G.; Bergenti, I.; Jaroń, T.; Ozarowski, A.; et al. Silver route to cuprate analogs. *Proc. Natl. Acad. Sci. USA* **2019**, *116*, 1495–1500. [CrossRef] [PubMed]
3. Mazej, Z.; Kurzydłowski, D.; Grochala, W. Unique Silver(II) Fluorides: The Emerging Electronic and Magnetic Materials. In *Photonic and Electronic Properties of Fluoride Materials: Progress in Fluorine Science Series*; Elsevier: Amsterdam, The Netherlands, 2016; pp. 231–260. ISBN 9780128017951.
4. Nilges, T.; Nilges, S.; Pfitzner, A.; Doert, T.; Böttcher, P. Structure−Property Relations and Diffusion Pathways of the Silver Ion Conductor Ag5Te2Cl. *Chem. Mater.* **2004**, *16*, 806–812. [CrossRef]
5. Adamczyk, W.; Połczyński, P.; Mika, A.; Jaroń, T.; Mazej, Z.; Fijalkowski, K.J.; Jurczakowski, R.; Grochala, W. New $Ag(F_{1-X}Cl_X)$ phases for energy storage applications. *J. Fluor. Chem.* **2015**, *174*, 22–29. [CrossRef]
6. Werner, W.; Strähle, J. The Crystal Structure of Silver Tetrachloroaurate(III) $AgAuCl_4$ and Its Crystal Chemical Relationship to the Rubidium Tetrachloroaurate(III) $RbAuCl_4$. *Z. Nat. B* **1977**, *32*, 741–744. [CrossRef]
7. Knies, M.; Anh, M.L.; Keßler, U.; Ruck, M. Crystal structures of the tetrachloridoaluminates(III) of rubidium(I), silver(I), and lead(II). *Z. Nat. B* **2020**, *75*, 117–123. [CrossRef]
8. Gaebell, H.-C.; Meyer, G.; Hoppe, R. Über Chloroargentate(I): $CsAgCl_2$ und schwarzes CsAgCl2+X. *Z. Anorg. Allg. Chem.* **1983**, *497*, 199–205. [CrossRef]
9. Hull, S.; Berastegui, P. Crystal structures and ionic conductivities of ternary derivatives of the silver and copper monohalides—II: Ordered phases within the $(AgX)_x{}^{-}(MX)_{1-X}$ and $(CuX)_x-(MX)_{1-x}$ (M = K, Rb and Cs; X = Cl, Br and I) systems. *J. Solid State Chem.* **2004**, *177*, 3156–3173. [CrossRef]
10. Hasselgren, C.; Jagner, S. Dirubidiumcatena-poly[dichloroargentate(I)-μ-chloro]. *Acta Crystallogr. Sect. C Cryst. Struct. Commun.* **1999**, *55*, 1208–1210. [CrossRef]
11. Bill, J.; Lerch, K.; Laqua, W. $Cs_2AgIAgIIICl_6$. Eine gemischtvalente Verbindung mit dreiwertigem Silber. *Z. Anorg. Allg. Chem.* **1990**, *589*, 7–11. [CrossRef]
12. Allen, J.; Scanlon, D.; Watson, G.W. Electronic structure of mixed-valence silver oxide AgO from hybrid density-functional theory. *Phys. Rev. B* **2010**, *81*, 1–4. [CrossRef]
13. McMillan, J. Magnetic properties and crystalline structure of AgO. *J. Inorg. Nucl. Chem.* **1960**, *13*, 28–31. [CrossRef]
14. Grzelak, A.; Gawraczyński, J.; Jaroń, T.; Somayazulu, M.; Derzsi, M.; Struzhkin, V.; Grochala, W. Persistence of Mixed and Non-intermediate Valence in the High-Pressure Structure of Silver(I,III) Oxide, AgO: A Combined Raman, X-ray Diffraction (XRD), and Density Functional Theory (DFT) Study. *Inorg. Chem.* **2017**, *56*, 5804–5812. [CrossRef]
15. Derzsi, M.; Grzelak, A.; Kondratiuk, P.; Tokár, K.; Grochala, W. Quest for Compounds at the Verge of Charge Transfer Instabilities: The Case of Silver(II) Chloride. *Crystals* **2019**, *9*, 423. [CrossRef]
16. Derzsi, M.; Uhliar, M.; Tokár, K. Ag_6Cl_4: The first silver chloride with rare Ag6 clusters from an ab initio study. *Chem. Commun.* **2021**, *57*, 10186–10189. [CrossRef]
17. Zhang, W.; Oganov, A.R.; Goncharov, A.F.; Zhu, Q.; Boulfelfel, S.E.; Lyakhov, A.O.; Stavrou, E.; Somayazulu, M.; Prakapenka, V.B.; Konôpková, Z. Unexpected Stable Stoichiometries of Sodium Chlorides. *Science* **2013**, *342*, 1502–1505. [CrossRef]
18. Bu, H.; Zhao, M.; Zhou, H.; Du, Y. Unusual electronic and mechanical properties of sodium chlorides at high pressures. *Phys. Lett. A* **2016**, *380*, 1556–1561. [CrossRef]
19. Zhang, W.; Oganov, A.R.; Zhu, Q.; Lobanov, S.; Stavrou, E.; Goncharov, A. Stability of numerous novel potassium chlorides at high pressure. *Sci. Rep.* **2016**, *6*, 26265. [CrossRef] [PubMed]
20. Shannon, R.D. Revised effective ionic radii and systematic studies of interatomic distances in halides and chalcogenides. *Acta Crystallogr. Sect. A* **1976**, *A32*, 751–767. [CrossRef]
21. Sonnenberg, K.; Mann, L.; Redeker, F.A.; Schmidt, B.; Riedel, S. Polyhalogen and Polyinterhalogen Anions from Fluorine to Iodine. *Angew. Chem. Int. Ed.* **2020**, *59*, 5464–5493. [CrossRef] [PubMed]
22. Shen, G.; Wang, Y.; Dewaele, A.; Wu, C.; Fratanduono, D.E.; Eggert, J.; Klotz, S.; Dziubek, K.F.; Loubeyre, P.; Fat'Yanov, O.V.; et al. Toward an international practical pressure scale: A proposal for an IPPS ruby gauge (IPPS-Ruby2020). *High Press. Res.* **2020**, *40*, 299–314. [CrossRef]
23. Akahama, Y.; Kawamura, H. Pressure calibration of diamond anvil Raman gauge to 410 GPa. *J. Phys. Conf. Ser.* **2010**, *215*, 012195. [CrossRef]
24. Kresse, G.; Hafner, J. Ab initiomolecular dynamics for liquid metals. *Phys. Rev. B* **1993**, *47*, 558–561. [CrossRef] [PubMed]
25. Kresse, G.; Hafner, J. Ab initiomolecular-dynamics simulation of the liquid-metal–amorphous-semiconductor transition in germanium. *Phys. Rev. B* **1994**, *49*, 14251–14269. [CrossRef]
26. Kresse, G.; Furthmüller, J. Efficiency of ab-initio total energy calculations for metals and semiconductors using a plane-wave basis set. *Comput. Mater. Sci.* **1996**, *6*, 15–50. [CrossRef]
27. Kresse, G.; Furthmüller, J. Efficient iterative schemes forab initiototal-energy calculations using a plane-wave basis set. *Phys. Rev. B* **1996**, *54*, 11169–11186. [CrossRef] [PubMed]

28. Kresse, G.; Joubert, D. From ultrasoft pseudopotentials to the projector augmented-wave method. *Phys. Rev. B* **1999**, *59*, 1758. [CrossRef]
29. Perdew, J.P.; Ruzsinszky, A.; Csonka, G.I.; Vydrov, O.A.; Scuseria, G.E.; Constantin, L.A.; Zhou, X.; Burke, K. Restoring the Density-Gradient Expansion for Exchange in Solids and Surfaces. *Phys. Rev. Lett.* **2008**, *100*, 136406. [CrossRef] [PubMed]
30. Henry, L.; Svitlyk, V.; Garbarino, G.; Sifre, D.; Mezouar, M. Structure of solid chlorine at 1.45 GPa. *Z. Krist. Cryst. Mater.* **2019**, *234*, 277–280. [CrossRef]
31. von der Osten, W. Polarized Raman spectra of silver halide crystals. *Phys. Rev. B* **1974**, *9*, 789–793. [CrossRef]
32. Martina, I.; Wiesinger, R.; Schreiner, M. Micro-Raman Characterisation of Silver Corrosion Products: Instrumental Set Up and Reference. *e-Preserv. Sci.* **2012**, *9*, 1–8.
33. Hull, S.; Keen, D.A. Pressure-induced phase transitions in AgCl, AgBr, and AgI. *Phys. Rev. B* **1999**, *59*, 750–761. [CrossRef]
34. Grzelak, A.; Gawraczyński, J.; Jaroń, T.; Kurzydłowski, D.; Budzianowski, A.; Mazej, Z.; Leszczyński, P.J.; Prakapenka, V.B.; Derzsi, M.; Struzhkin, V.V.; et al. High-Pressure Behavior of Silver Fluorides up to 40 GPa. *Inorg. Chem.* **2017**, *56*, 14651–14661. [CrossRef] [PubMed]
35. Johannsen, P.G.; Holzapfel, W.B. Effect of pressure on Raman spectra of solid chlorine. *J. Phys. C Solid State Phys.* **1983**, *16*, L1177–L1179. [CrossRef]
36. Lockwood, D.J.; Bertrand, D.; Carrara, P.; Mischler, G.; Billerey, D.; Terrier, C. Raman spectrum of $NiCl_2$. *J. Phys. C Solid State Phys.* **1979**, *12*, 3615–3620. [CrossRef]
37. McGuire, M.A.; Yan, J.; Lampen-Kelley, P.; May, A.F.; Cooper, V.R.; Lindsay, L.; Puretzky, A.; Liang, L.; Kc, S.; Cakmak, E.; et al. High-temperature magnetostructural transition in van der Waals-layered $\alpha-$MoCl3. *Phys. Rev. Mater.* **2017**, *1*, 064001. [CrossRef]
38. Kazim, S.; Ali, M.; Palleschi, S.; D'Olimpio, G.; Mastrippolito, D.; Politano, A.; Gunnella, R.; Di Cicco, A.; Renzelli, M.; Moccia, G.; et al. Mechanical exfoliation and layer number identification of single crystal monoclinic $CrCl_3$. *Nanotechnology* **2020**, *31*, 395706. [CrossRef]
39. Somayazulu, M.; Gramsch, S.; Mao, H.-K.; Hemley, R. High Pressure-High Temperature Reactions in Xenon-Chlorine System. In *Proceedings of the MRS Proceedings*; Springer Science and Business Media LLC: Berlin/Heidelberg, Germany, 2006; Volume 987.
40. Chaney, J.; Feigerle, C. Characterization of chlorinated chemical vapor deposited and natural (100) diamond. *Surf. Sci.* **1999**, *425*, 245–258. [CrossRef]
41. Pravica, M.; Sneed, D.; Wang, Y.; Smith, Q.; Subrahmanyam, G. Carbon tetrachloride under extreme conditions. *J. Chem. Phys.* **2014**, *140*, 194503. [CrossRef] [PubMed]
42. Brückner, D.C.R.; Haller, D.C.H.; Ellwanger, M.; Riedel, S. Polychloride Monoanions from $[Cl_3]-$ to $[Cl_9]-$: A Raman Spectroscopic and Quantum Chemical Investigation. *Chem. A Eur. J.* **2012**, *18*, 5741–5747. [CrossRef] [PubMed]
43. Brückner, R.; Haller, H.; Steinhauer, S.; Müller, C.; Riedel, S. A 2D Polychloride Network Held Together by Halogen-Halogen Interactions. *Angew. Chem. Int. Ed.* **2015**, *54*, 15579–15583. [CrossRef] [PubMed]
44. Haller, H.; Riedel, S. Recent Discoveries of Polyhalogen Anions—From Bromine to Fluorine. *Z. Anorg. Allg. Chem.* **2014**, *640*, 1281–1291. [CrossRef]
45. Uhliar, M.; Tokár, K.; Kohulák, O.; Derzsi, M. Exploring crystal chemistry of binary silver chlorides with evolutionary algorithms and density functional theory. In Proceedings of the 2nd International Online Conference on Crystals, Online, 10–20 November 2020; MDPI: Basel, Switzerland, 2020.